POLITECNICO DI TORINO
Repository ISTITUZIONALE

Three-dimensional printed polymeric system to encapsulate human mesenchymal stem cells differentiated into islet-like insulin-producing aggregates for diabetes treatment

Original
Three-dimensional printed polymeric system to encapsulate human mesenchymal stem cells differentiated into islet-like insulin-producing aggregates for diabetes treatment / Sabek, O.M., Farina, M., Fraga, D.W., Afshar, S., Ballerini, A., Filgueira, C.S., Thekkedath, U.R., Grattoni, A., Gaber, O.. - In: JOURNAL OF TISSUE ENGINEERING. - ISSN 2041-7314. - 6: 1–13:(2016). [10.1177/2041731416638198]

Availability:
This version is available at: 11583/2674121 since: 2017-06-07T04:09:33Z

Publisher:
Sage

Published
DOI:10.1177/2041731416638198

Terms of use:

This article is made available under terms and conditions as specified in the corresponding bibliographic description in the repository

Publisher copyright

(Article begins on next page)

18 November 2026

Original Article

Journal of Tissue Engineering
Volume 7: 1–13
© The Author(s) 2016
Reprints and permissions:
sagepub.co.uk/journalsPermissions.nav
DOI: 10.1177/2041731416638198
tej.sagepub.com
SAGE

Three-dimensional printed polymeric system to encapsulate human mesenchymal stem cells differentiated into islet-like insulin-producing aggregates for diabetes treatment

Omaima M Sabek[1], Marco Farina[2,3], Daniel W Fraga[1], Solmaz Afshar[1], Andrea Ballerini[2,4], Carly S Filgueira[2], Usha R Thekkedath[2], Alessandro Grattoni[2] and A Osama Gaber[1]

Abstract

Diabetes is one of the most prevalent, costly, and debilitating diseases in the world. Pancreas and islet transplants have shown success in re-establishing glucose control and reversing diabetic complications. However, both are limited by donor availability, need for continuous immunosuppression, loss of transplanted tissue due to dispersion, and lack of vascularization. To overcome the limitations of poor islet availability, here, we investigate the potential of bone marrow–derived mesenchymal stem cells differentiated into islet-like insulin-producing aggregates. Islet-like insulin-producing aggregates, characterized by gene expression, are shown to be similar to pancreatic islets and display positive immunostaining for insulin and glucagon. To address the limits of current encapsulation systems, we developed a novel three-dimensional printed, scalable, and potentially refillable polymeric construct (nanogland) to support islet-like insulin-producing aggregates' survival and function in the host body. In vitro studies showed that encapsulated islet-like insulin-producing aggregates maintained viability and function, producing steady levels of insulin for at least 4 weeks. Nanogland—islet-like insulin-producing aggregate technology here investigated as a proof of concept holds potential as an effective and innovative approach for diabetes cell therapy.

Keywords

Human bone marrow, mesenchymal stem cells, diabetes, polylactic acid, scaffold, three-dimensional printer

Received: 31 October 2015; accepted: 18 February 2016

Introduction

Diabetes is an epidemic estimated by the International Diabetes Federation to affect more than 415 million people worldwide.[1] Diabetes mellitus, a disease caused by either reduced insulin production due to autoimmune eradication of pancreatic β-cells (type 1) or peripheral insulin resistance (type 2), eventually results in severe hyperglycemia, organ failure, and increased morbidity, and, possibly, mortality.[2] Failure in glucose homeostasis can result in various auxiliary complications such as cardiovascular disease, and according to the Centers for Disease Control and Prevention, it is the main cause of kidney failure, blindness, and amputations.[3,4] The current standard of care for type 1 diabetes patients involves

[1]Department of Surgery, Houston Methodist Hospital, Houston, TX, USA
[2]Department of Nanomedicine, Institute for Academic Medicine, Houston Methodist Research Institute, Houston, TX, USA
[3]Department of Electronics and Telecommunications, Politecnico di Torino, Torino, Italy
[4]Department of Biotechnology and Translational Medicine, The University of Milan, Milan, Italy
Omaima M Sabek and Marco Farina contributed equally to this work.

Corresponding authors:
Alessandro Grattoni, Department of Nanomedicine, Institute for Academic Medicine, Houston Methodist Research Institute, 6670 Bertner Street, Houston, TX 77030, USA.
Email: agrattoni@houstonmethodist.org

A Osama Gaber, Department of Surgery, Houston Methodist Hospital, 6550 Fannin Street, Houston, TX 77030, USA.
Email: AOGaber@houstonmethodist.org

Creative Commons Non Commercial CC-BY-NC: This article is distributed under the terms of the Creative Commons Attribution-NonCommercial 3.0 License (http://www.creativecommons.org/licenses/by-nc/3.0/) which permits non-commercial use, reproduction and distribution of the work without further permission provided the original work is attributed as specified on the SAGE and Open Access pages (https://us.sagepub.com/en-us/nam/open-access-at-sage).

daily monitoring of blood glucose levels and the continuous injection of insulin,[5] and for patients with type 2 diabetes, oral or injected therapeutics. Both treatments have their respective side effects including ketosis and hypoglycemic coma. It is widely accepted that therapies aimed at regeneration or replacement of damaged insulin-producing β-cells could be a more permanent cure for treating diabetes. Pancreas and islet transplants have shown success at re-establishing glucose control and reversing diabetic complications, but their routine clinical application is still inadequate, primarily due to the limited supply of cadaveric organs and loss of graft function over time due to immune rejection, lack of neovascularization, and loss of physiological architecture. Patients transplanted with cadaveric human islets can become insulin independent for about 5 years, but limited quantity and quality of donor islets make it an unrealistic cure.[6,7] The ideal therapy would restore insulin from autologous cell populations. The discovery of pluripotent stem cells, which have the capability of evolving to any cell type, has inspired the use of these cells for disease treatment and drug screening.[8] The ability to produce an unlimited supply of islet-like insulin-producing aggregates (ILIPAs) from stem cells, and the subsequent transplantation to easily accessible sites, could result in a permanent cure to millions of patients affected by diabetes. In order to support the long-term survival and function of these transplanted cells in the host body and to protect them from dispersion, destruction, and immunological attack, several micro- and macroencapsulation and delivery strategies have been tried with varied results.[9] Polylactic acid (PLA) is widely used in many different biomedical applications due to its biocompatibility, biodegradability, and non-toxic degradation products.[10] Its long half-life, which may not be desirable in other biomedical applications, is advantageous in designing long-term implantable devices like cell encapsulation systems for diabetes. Furthermore, it is possible to modify the surface structure and properties of PLA through different techniques, allowing better biomimetic properties useful to improve its application as a cell reservoir scaffold for cells of different origins.[11] In this study, we characterize differentiated ILIPAs from adult human bone marrow–derived mesenchymal stem cells (BM-MSCs) and compare their genetic signatures to pancreatic human islets. We also develop a three-dimensional (3D) printed PLA delivery and encapsulation system suitable for possible subcutaneous implantation of pancreatic cells.

Materials and methods

Human pancreatic islets isolation and purification

Human pancreata (n = 5) were obtained from heart-beating donors deceased by brain death with informed consent for transplant or research use from relatives of the donors. Human islets were isolated from cadaver donors using an adaptation of the automated method described by Ricordi et al.[12] See supplementary files for more details.

Islet cell culture

Aliquots from human islet isolations were then cultured in Memphis serum-free medium (M-SFM) further supplemented with 10 U/mL of heparin and 10 mM of niacin as described previously.[13] Islet culture medium was changed at day 1 post-isolation and thereafter weekly for all islet preparations during the culture period. Islet tissue was cultured for 1–3 days prior to experimentation, to allow for sterility and viability testing. These islets were used as positive controls for BM-MSC-derived ILIPAs.

Isolation, expansion, and differentiation of BM-MSCs

Bone marrow samples (n = 5) were recovered from leftover tissue in used bone marrow collection bag sets, properly consented for research utilization. The age of the bone marrow donors ranges from 21–55 years. Isolation, expansion, and differentiation of BM-MSCs were performed according to the procedures outlined by Gabr et al.[14] See supplementary file for more details.

Characterization of isolated mesenchymal stem cells by flow cytometry

For flow cytometric analysis, the mesenchymal stem cells (MSCs) at passage three were trypsinized, centrifuged at 300 g for 8 min, and resuspended in phosphate-buffered saline (PBS) at a concentration of 1×10^6 cells/mL. A total of 100 µL of aliquots were labeled for 30 min with antibodies against CD14, CD45 (fluorescein isothiocyanate (FITC)), or CD73; CD34 phycoerythrin (PE; Becton Dickinson, USA); or CD106, CD29 PE, or CD44 (FITC; Becton Dickinson), washed with 1 mL of stain buffer (BD-Pharmingen, USA) and resuspended in 500 µL of stain buffer. The labeled cells were analyzed using an argon-ion laser with a wavelength of 488 nm (FACS Calibur; Becton Dickinson). A total of 10,000 events were obtained and analyzed with the DIVA software program (Becton Dickinson). Control staining with appropriate isotype-matched monoclonal antibodies was included.

Differentiation of the MSCs to ILIPAs

After passage three, MSCs with appropriate CD profiles were seeded at a density of 1×10^5 cells/mL in serum-free, high-glucose (450 mg/dL) Dulbecco's Modified Eagle's medium (D-MEM; 25 mmol/L) containing 0.5 mmol/L of β-mercaptoethanol (Sigma) and incubated for 2 days. The

medium was replaced with serum-free, glucose-rich medium containing 1% nonessential amino acids (Sigma), 20 ng/mL basic fibroblast growth factor (Sigma), 20 ng/mL epidermal growth factor (Sigma), 2% B27 supplement (Gibco BRL, Life Technologies, UK), and 2 mmol/L L-glutamine (Sigma). The preparations were cultured for 8–10 days. Finally, the cells were cultured for an additional 8–10 days in serum-free, high-glucose D-MEM containing 10 ng/mL betacellulin (Sigma), 10 ng/mL activin-A (Sigma), 2% B27 supplement, and 10 mmol/L nicotinamide (Sigma).

Immunolabelling

Immunohistochemistry was performed using primary antibodies against insulin (AB6995; Abcam, Cambridge, MA) and glucagon (AB92517; Abcam). For nanogold immunostaining, the ILIPAs were fixed in 2% formalin and 0.5% glutaraldehyde (EM grade from Ted Pella) in PBS overnight at 4°C. After washing 3 × 15 min with PBS containing 0.05% Tween 20 (Bio-Rad Laboratories, Hercules, CA, USA), ILIPAs were blocked for 6 h in casein blocking buffer (Bio-Rad Laboratories) with 0.05% Tween 20 at room temperature. Subsequently, samples were incubated with mouse monoclonal anti-c-peptide (1H8) antibody (Abcam, ab8297) at 1:50 dilution in blocking buffer, overnight at 4°C. The next day, samples were washed for several hours with 0.05% PBS Tween 20 and incubated overnight at 4°C with anti-mouse antibody conjugated with 1.4 nm gold (Nanoprobes, Yaphank, NY, USA) diluted at 1:50 with blocking buffer. The next day, samples were washed 3 × 15 min with 0.05% PBS Tween 20, post-fixed for 20 min in 1% glutaraldehyde in 0.05% PBS Tween 20, washed 3 × 15 min in water, silver enhanced, and either photographed as a whole mount or processed for electron microscopy without the osmium tetraoxide treatment, as described previously. Whole-mount immunostained ILIPAs were contrasted with 0.5% uranyl acetate only (without osmium tetraoxide) and embedded in Epon. Thin (70–100 nm) sections were examined and photographed in JEOL 1200 transmission electron microscope.

Microarray analysis

RNA was extracted using the Trizol Hybrid RNA Method, RNA quality assessed with the Agilent Bioanalyzer, and RNA samples amplified using the Ambion WT Expression Kit (Affymetrix). Fragmentation/terminal-labeled RNA was hybridized to the Affy 1.1ST human chip and processed with the GeneTitan system.

Gene expression by reverse transcription–polymerase chain reaction

Total RNA (totRNA) was extracted in accordance with the manufacturer's instructions. Variable amounts of total RNA input were reverse transcribed using the iScript cDNA Synthesis Kit (Bio-Rad Laboratories), the amount defined by the respective samples' concentration (from 5 to 1000 ng total RNA input).

TaqMan® (Life Technologies) analysis was performed on the Roche LightCycler 480 II Instrument with LightCycler® 480 Probes Master mix (Roche). See supplementary Table 2 for the list of TaqMan primers/probes analyzed. For more representative normalization, a cDNA master mix (cDNA, 2X Probes master mix, polymerase chain reaction (PCR)-grade water) was prepared for each cDNA sample to which either query or normalizing TaqMan primers/probe was subsequently added. This procedure allows the query and normalizing primers/probe to interrogate the same cDNA master mix preparation, resulting in more accurate normalization.[15] Normalized Cp values (critical point; Cp_{query}—geometrix-mean ($Cp_{PPIA,}$ Cp_{18S})) were analyzed. In addition, relative quantitative reverse transcription–polymerase chain reaction (RT-PCR) (quantitative polymerase chain reaction (qPCR)) gene expression for differentiated islet-like pancreatic cells were analyzed against human islets served as a positive control and acinar and undifferentiated MSCs as a negative control.

Nanogland fabrication

For nanogland (NG) fabrication, we used a 3D printer (Makerbot 2X; Makerbot Industries New York, USA). This 3D printer runs on fused deposition modeling (FDM) technique, building parts layer-by-layer from the bottom-up by heating and extruding thermoplastic filament. A solid modeling software (SolidWorks®, Dassault Systèmes SolidWorks Corp.) was used to create a 3D dataset for the fabrication process. Biocompatible PLA (Foster Corporation, CT, USA) was used to fabricate the NGs (Figure 5).

The NG consists of a cell reservoir (250μL) and has a discoidal shape with a diameter of 13 mm and a thickness of 4.5 mm. The cell reservoir consists of an array of microchambers (200 μm × 200 μm) to house each pancreatic islet or ILIPA individually. The microchambers are connected to the outside by an array of square microchannels (150 μm × 150 μm cross section and 50 μm length).

NG surface patterning and modification

After fabrication, NG surface modification was performed, using various agents as described below to obtain suitable external charge and hydrophilicity for supporting cell growth and viability. All of the PLA NGs were immersed in a 5-M NaOH (Macron Chemicals, PA, USA) solution in Millipore water for 4 h under mild agitation, then rinsed, and dried at room temperature. A NG custom holder has been fabricated for running two 60-s cycles of argon

plasma (Ar) or oxygen plasma (O_2) etching (30 W, 150 mTorr) (March plasma etcher, Nordson, OH, USA).

Five NGs were placed in a petri dish filled with a poly-L-lysine (PLL) solution 0.01%, 150,000–300,000 MW (PLL, Sigma Aldrich), incubated for 5 min, and air dried at room temperature. The second group of five NGs was placed in a petri dish filled with endothelial cell attachment factor (ECAF; Sigma Aldrich, sterile-filtered liquid), followed by a 10-min incubation, and dried at room temperature, as per manufacturer's instructions.

Stability of surface modification in vitro

All surface-modified NG groups were immersed in PBS for 40 days under gentle agitation at 37°C. NG surface conformation and water contact angle were measured at different time points (1, 3, 7, 14, 21, 28, and 40 days), and the images were analyzed using ImageJ software.

Cell viability in surface-modified NGs in vitro

For the in vitro cell viability study, flat PLA membranes (n = 7) were printed (20 mm diameter, 1 mm thickness); treated with NaOH, argon plasma, PLL, and ECAF (n = 6 per each group); assembled into 6-well polystyrene cell culture inserts (Becton Dickinson); and filled with 1.5×10^5 human umbilical vein endothelial cells (HUVECs) in a volume of 1 mL of complete endothelial cell basal medium (EBM, Lonza, USA). All samples were incubated at 37°C and 5% CO_2 for 7 days with a change of media at regular time intervals (2, 4, and 7 days). To assess viability, cells were rinsed with PBS buffer, trypsinized (trypsin/ethylenediaminetetraacetic acid (EDTA) solution), and quantified using Trypan blue solution.

Assessment of insulin secretion and content in vitro

Standard aliquots of 50 islets equivalent (IEQ) or 100 IEQ of ILIPAs were incubated for 60 min with low glucose (60 mg/dL, basal), followed by 60 min of high glucose (300 mg/dL, stimulated).[16] Following high-glucose incubation, islets were harvested and insulin was extracted in an ethanol–acid solution (165 mM HCl in 75% ethanol). The islets were then analyzed for insulin content using a specific enzyme-linked immunosorbent assay (ELISA) assay (ALPCO Diagnostics, Windham, NH). The low-glucose medium used was standard alpha MEM supplemented with 5% platelet lysate (PL). The high-glucose stimulation medium was high-glucose D-MEM (450 mg/dL glucose) supplemented with 5% PL.

ILIPAs insulin secretion in NG

In order to assess the long-term viability of ILIPAs when housed in the NG device, we loaded multiple NGs (10 per group) with approximately 2000 ILIPA constructs. The ILIPAs were loaded in a PL gel into the NG. Briefly, NGs were placed in the wells of a sterile 12-well suspension type plate (Sarstedt). ILIPAs were centrifuged and medium was removed. The ILIPAs were mixed with PL at a concentration that would allow for approximately 2000 ILIPAs to be loaded in a volume of 200 µL (10,000 ILIPAs/mL). Three NG treatment types were tested in this evaluation: NGs without surface modification (untreated), NGs' surface modified with argon plasma, and NGs' surface modified with oxygen plasma. Once the PL-ILIPAs were loaded into the wells, 50 µL of thrombin (2000 units/mL; King Pharma, Bristol, TN) was mixed with the solution. The plates were placed in a 37°C, 5% CO_2 incubator for 60 min to allow complete formation of the gel.

Once gelation was accomplished, the NGs were transferred into new microplates and 3 mL of alpha MEM with 5% PL was added to the wells. The medium was replaced every 3–4 days for the next month. The NGs were tested weekly for insulin release using a perifusion-type evaluation.

On days 7, 14, 21, and 28, the medium was collected from the NG wells and saved for insulin analysis. The medium was replaced with fresh medium that represented the low-glucose portion of the testing (100 mg/dL). The plates were incubated for 30-min intervals, and the medium was harvested for insulin analysis every 30 min for up to 6 h. The medium was changed to high-glucose medium at 90 min and remained so until the final incubation of the day. At this time, the medium was replaced with low-glucose medium, and the plates were returned to the incubator overnight. The following morning, medium was collected and again replaced with high-glucose medium, with incubation extending up to another 3–4 h.

Statistical analysis

Results are expressed as means and standard deviations for at least three replicates. One-way nonparametric analysis of variance followed by Tukey's post hoc test was assessed to verify statistical significance; $p < 0.05$ was considered statistically significant. Statistical analysis was performed using Prism 5 software (GraphPad Software Inc., San Diego, CA, USA).

Results

Morphological and phenotypical characterization of the cultured MSCs

At the end of the expansion phase, the cells became homogenous, spindle shaped, fibroblast-like and arranged in monolayers (Figure 1c). Flow-cytometric analysis showed that they expressed high percent levels of CD29 (80.4±17.1), CD44 (47.8±25.8), and CD106 (10±19.5), but negligible levels of CD14 (1±1.5), CD34 (2.7±1.7) and

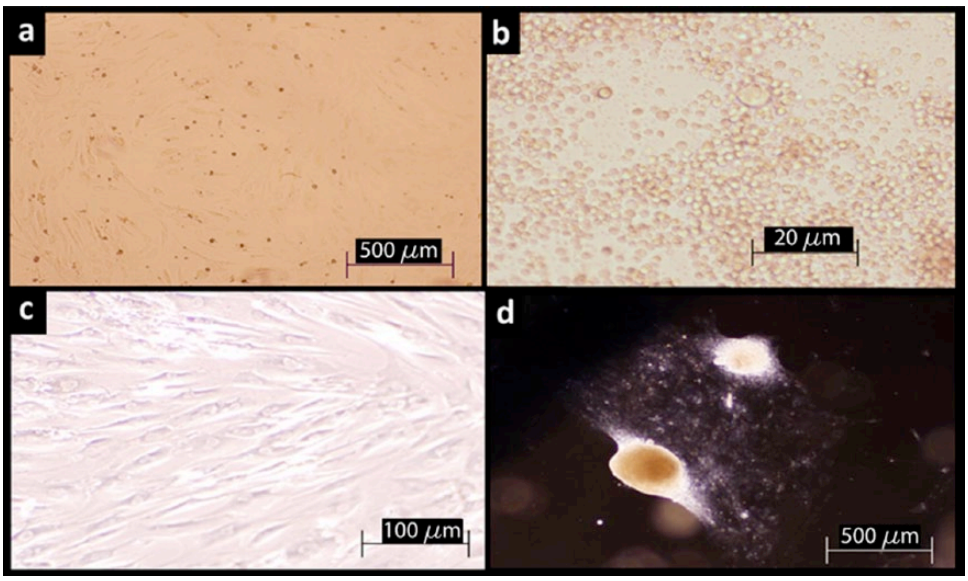


Figure 1. Morphological changes of bone marrow–derived cells (MSCs) differentiated into functional islet-like structures (ILIPAs): (a) bone marrow cells; (b) purified MSC; (c) undifferentiated MSCs, at the end of the expansion phase; and (d) contrast phase microscopy showing aggregation of differentiating MSCs into insulin-producing ILIPA.

CD45 (7.6±6.9). These results indicate that majority of the bone marrow-derived cells were MSCs and that the number of MSC obtained at the end of the expansion phase varies from one donor to another.[17] During the MSC differentiation into ILIPA phase, cells gathered gradually in groups with the formation of three-dimensional aggregates. At the end of the differentiation protocol, cells formed clusters with spheroidal morphology (Figure 1). A difference in the rate of growth or differentiation was observed between different donors (data not showed).

At the end of differentiation, immunofluorescent labeling and electron microscopy demonstrated c-peptide positive staining in the differentiated ILIPAs.

Furthermore, using immunohistochemistry we show that differentiated ILIPAs contain α-cells that are positively stained for glucagon and β-cells positively stained for insulin (Figure 2 and Supplementary Figure 1).

Gene expression profile of human pancreatic islets and ILIPAs

Human islets ($n = 5$) and ILIPAs ($n = 5$) were analyzed for gene profile using high-density Affymetrix U133A Gene Chips (analyzed by Gene Spring software). Genes that met the criteria for statistically significant differential expression ($p \leqslant 0.01$) at false discovery rate of 2% were identified by Welch's t-test. This list was further refined by omitting those genes whose fold-difference of expression was less than two. Using Ingenuity Pathways Analysis software, we identified differential gene expression profiles in islets that play a role in insulin synthesis and secretion as well as glucose metabolism (Supplementary Table 1 and Figure 3). While there was no difference in the insulin expression between islets and ILIPAs, islets had high relative levels of genes that promote insulin production and secretion, such genes included ABCC8, PDX1, RFX6 PCSK1, SLC2A2, FOXA2, and SST.

RT-PCR of differentiated ILIPAs

Islet gene expression profile varies in different donors. To determine the variation in gene expression profile of different ILIPA preparations, we examined five differentiated ILIPA preparations and compared them to an average of five human islet preparations as a positive control and to undifferentiated MSCs and acinar cells as a negative control. We tested for genes that are crucial for insulin secretion and glucose metabolism and results expressed by previous gene expression array, such as Insulin, SST, ABCC8, SC2A2, PDX1, FOXA2, RFX6, and PSCK1. As shown in Figure 4, there is a wide variation between different ILIPA preparations, where two out of five have similar expression levels as the islets.

NG surface treatment and endothelial cell culture

Different surface treatments were tested to augment PLA NG hydrophilicity (Table 1; Figure 5). All of the tested surface modifications reduce water contact angle on the polymer surface in the first week after treatment. The effect was higher when the NGs were treated with a combination of Ar plasma and ECAF ($p < 0.001$), but this group

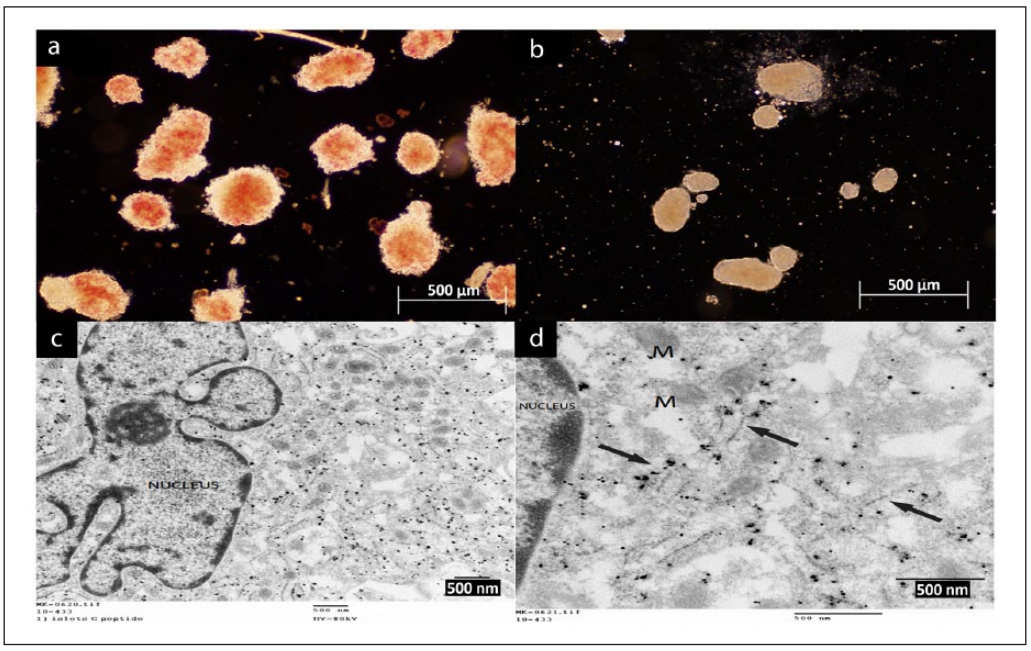


Figure 2. Differentiated ILIPAs (b) are similar in size to human islets (a). ILIPA EM photomicrograph (d) stained with gold nanoparticles labeled with antibodies to C-peptide (black arrows) at the cisternae of rough endoplasmic reticulum (c) and (d).

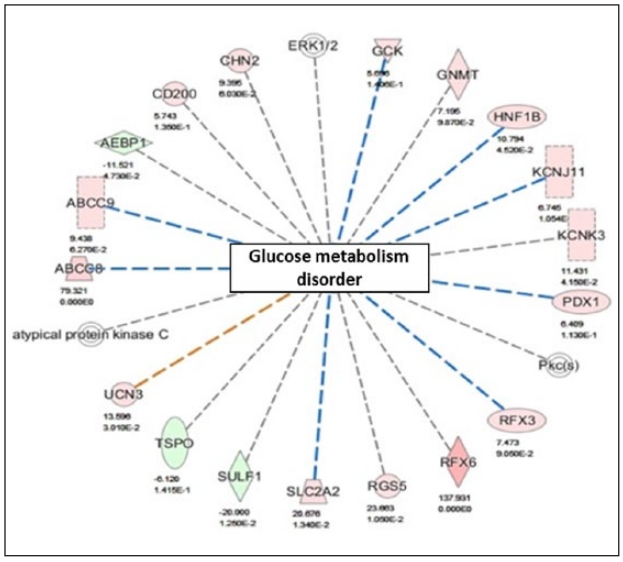


Figure 3. Glucose metabolism disorder network generated using Ingenuity Pathways Analysis software comparing human islets to ILIPAs. Upregulated genes are shown in red and downregulated genes in green. Genes that are important to glucose metabolism such as ABCC8, RFX6, and SLC2A2 are expressed much higher in the islets with fold changes of 79, 138, and 21, respectively.

lost the hydrophilic change in almost 1 week, becoming comparable to the other treated groups. All the groups treated with Ar plasma maintained the surface characteristics, as shown by low contact angle at 1 month from the surface treatment ($p < 0.01$), but only the combination with PLL and ECAF maintained the effectiveness at day 40 ($p < 0.05$) (Figure 6).

Cell proliferation and viability were tested in surface-modified NGs using HUVECs. HUVECs were grown on NGs treated with PLL and Ar. Plasma treatment showed a slower growth compared to all the other surface treatments ($p < 0.05$). All groups cultured in surface-treated NGs showed a mean viability higher than 90%, and dimension comparable to control, with minor differences between the control and untreated NGs (16.81 vs 15.54 µm, $p < 0.05$). All cells cultured inside the NGs grew slower than the control group cultured in classical polystyrene well ($p < 0.001$) (Figure 7).

Insulin secretion by ILIPAs in NG

A month-long ILIPA culture was conducted in polymeric NGs with different surface treatments to understand long-term viability and insulin secretion in response to glucose stimuli.

ILIPAs showed an ability to produce steady levels of insulin throughout the testing process. The insulin accumulated in the testing media in a consistent manner showing spikes in insulin production and accumulation at time 0 (following weekend incubation) as well as following overnight incubation during the testing. These spikes seem constant during the entire duration of study, with a statistically non-significant reduction trend during week 4 in all groups. There were no differences in both basal insulin secretion and response to high glucose in argon- or oxygen-treated NGs. ILIPAs showed no significant difference in overall performance over the testing period when different types of surface treatments

Table 1. Water contact angle of PLA after different surface treatments.

	Day 0	Day 1	Day 10	Day 30	Day 40
Control	74.92 (3.43)	73.25 (2.02)	72.75 (3.88)	72.10 (3.23)	67.61 (3.93)
Ar	39.95 (5.76)	40.05 (1.54)	40.25 (4.11)	51.32 (1.35)	69.29 (1.14)
Ar + PLL	53.41 (2.35)	52.65 (5.51)	45.10 (3.57)	49.22 (2.46)	57.54 (3.63)
Ar + ECAF	8.27 (6.72)	20.00 (5.35)	41.20 (6.23)	51.41 (5.32)	58.12 (5.56)

PLA: polylactic acid; Ar: argon plasma; PLL: poly-L-lysine; ECAF: endothelial cell attachment factor.

were compared and insulin release tracking was consistent for each NG cohort (Figure 8).

When comparing ILIPAs in the NG-PL to free ILIPAs tested in the same manner, we see a rapid drop in insulin levels for the free ILIPAs compared to those in the NG devices, presumably due to retention of insulin within the PL gel matrix (Figure 8(a)).

Discussion

Over the last few decades, islet and stem cell transplantation has been explored as a promising method to achieve strict control of blood glucose and as a potential cure for diabetes. Two key problems for these cell therapies are the lack of adequate islets or islet-like tissue and the need to use immunosuppressants. Here, we develop a new, alternative advanced cell therapy for diabetes based on human MSCs. MSCs are multipotent stromal cells with the ability to proliferate and differentiate into a variety of cell types including insulin-producing cells. Since MSCs comprise only 0.001% to 0.01% of bone marrow mononuclear cells,[17–20] in vitro expansion of these cells is necessary to obtain sufficient cell numbers for clinical use. Following the expansion phase, cells were driven to differentiate into ILIPAs that express pancreatic islet genes and secrete insulin. The premise of stem cell therapy for diabetes is the production of autogenous differentiated cells that mimic pancreatic islets and β-cells as a source of insulin for blood glucose homeostasis.[17] Our data show that despite the success in creating ILIPAs that are capable of insulin and C-peptide production, there was a variation among cultures from different donors in key transcriptional factor expression such as PDX1, a factor responsible for the development of the pancreas in humans as well as maintaining insulin gene expression and β-cell survival. Down regulation in the expression of PDX1 could lead to β-cell failure and subsequently type 2 diabetes.[21] RFX6 was another transcription factor upregulated in ILIPAs, commonly responsible for the regulation of insulin gene expression and secretion and is thought to be involved in islet cell differentiation.[22]

ILIPAs expressed SLC2A2, a gene that produces GLUT2, the specific glucose transporter in β-cells, responsible for glucose homeostasis by enabling transport across cell membranes, tuning insulin secretion,[23] PCSK1, proprotein convertase subtilisin kexin type 1 (PCSK1), which belongs to the subtilisin-like proprotein convertase family that process latent precursor proteins, such as proinsulin, into their biologically active products, and ABCC8, a gene included ATP-binding cassette, sub-family C (CFTR/MRP), member 8, which functions as a modulator of ATP-sensitive potassium channels and insulin release.[24,25] Donor variability is a major concern. Our laboratory found that not all donor cells differentiate at the expected time frame; indeed some took a longer time to reach the desired phase. This variability could be due to differences in age and gender.[26] Therefore, testing ILIPA preparation with RT-PCR for key genes required for healthy islet function could be essential for possible future clinical studies. RNA-sequencing could be a valid method to further characterize ILIPA gene expression and their biological characteristics, which will require larger quantity of cells. For future experiments, we plan to expand the production of ILIPAs to be able perform several different analyses.

As reported from the outcomes of currently used clinical protocols for islet transplantation, such as the Edmonton protocol, intraportal pancreatic injection does not offer an ideal physiological environment for pancreatic islet engraftments, and their viability is hampered by acute hypoxia after transplantation.[27] A possible way to overcome this limitation is to house pancreatic islets and cells in a system able to provide mechanical support, immunological protection, easy passage of nutrients and oxygen to meet the high metabolic demand, while keeping the ability to rapidly respond to plasma glucose changes in an adequately vascularized subcutaneous environment. It is possible to fabricate such tridimensional biomimetic encapsulation systems using low-cost and customizable 3D printers able to print medical grade synthetic polymeric material as well as biological tissue to better reproduce normal physiology. To enhance the long-term efficacy of islet transplantation by improving vascularization while reducing immunogenicity, a tissue engineering approach of 3D culturing insulin-producing cells encapsulated in NGs could be implemented by filling a bioreactor's interior with a biomimetic extracellular matrix (ECM)-like scaffold and seeding with pancreatic β-cells or islets.

Implantable biocapsules have been proposed as a promising approach for transplanting cells and protecting them from immune rejection.[28] Ferrari et al. demonstrated that silicon based cell biocapsules have the advantage of mechanical strength and biochemical inertness.[29,30]

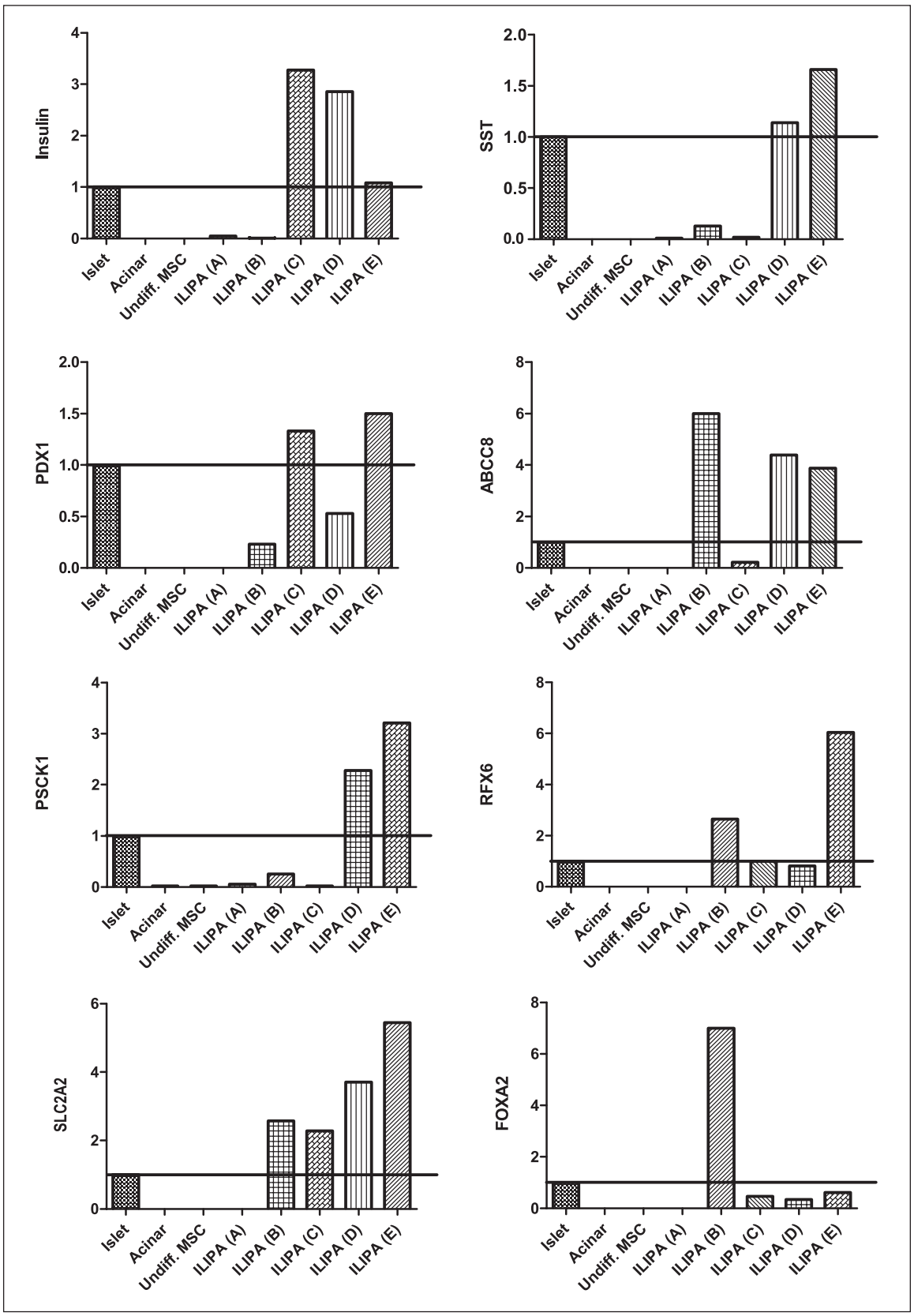


Figure 4. Real-time PCR of islet's key transcription factors expression of acinar cells, undifferentiated MSC, and differentiated ILIPAs from five different donors, normalized to five different isolated human islets. The results are expressed as the fold change difference of islets to ILIPAs.

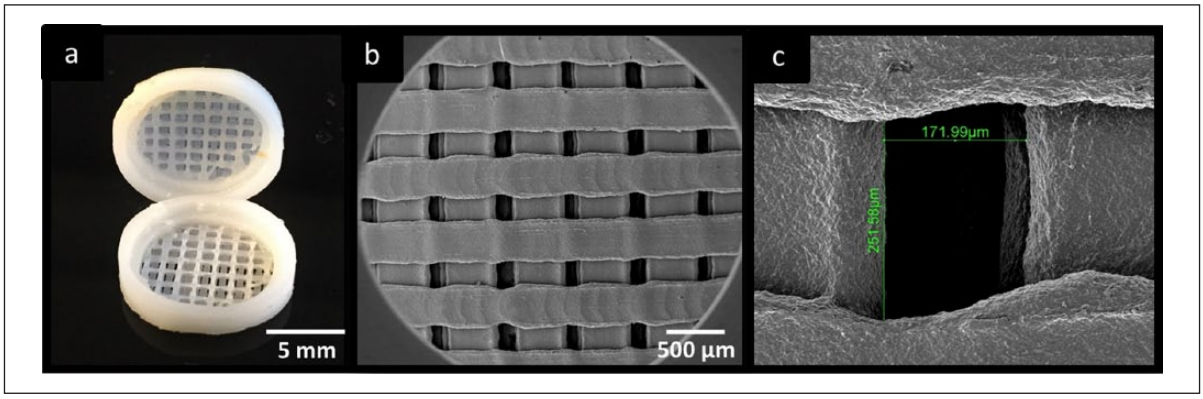


Figure 5. (a) An open section of a 3D printed PLA nanogland showing cell chambers and microchannels; (b) and (c) SEM images of the array of microchambers.

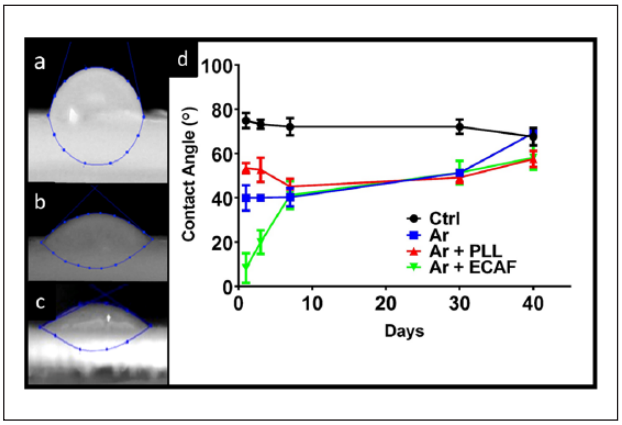


Figure 6. Comparison of hydrophilicity achieved by various surface modification techniques, as measured by water contact angle on day 1 (a = control, b = PLL, c = ECAF) and their stability over 40 days.

Silicon membranes were microfabricated with photolithographic techniques allowing for fine control over pore size and distribution in the 20–100 nm range.[31]

Our group is developing a NG system composed of biocompatible silica or polymeric encapsulation with insulin-producing cell clusters contained in a 3D biological matrix providing the ability to replace physiological function of native islets for diabetes treatment.

In previous work, we demonstrated that a silicon microfabricated device, composed by channels ranging from 3.6 nm to 60 µm filled with pancreatic islets, showed good glucose response and insulin release in vitro and in vivo.[29] This "silicon pancreas" provided immunological protection and mechanical support for islet growth, but it showed limited angiogenic potential and metabolic diffusion when implanted subcutaneously in mice.

To overcome these limits and achieve customization and scalability, we developed a new 3D printed NG using biocompatible functionalized polymers, fillable with ECM-like PL gel matrix to better nurture the pancreatic islets or other insulin secreting cells, such as ILIPAs, derived by MSCs or other sources.[32]

Our NGs offer easy evaluation for the role of angiogenesis and vascularization on insulin production, glucose stimulation, and cell viability and provide co-culturing options for pancreatic cells with endothelial cells or other vascular progenitor cells.

Furthermore, to address one-by-one all of the pitfalls of commonly used pancreatic cell bioreactors and macroencapsulation systems, it is possible to functionalize the polymeric scaffold, to induce local angiogenesis or endothelial migration, improve islets' metabolic function, and reduce the risk of immunological rejection. Indeed, surface characteristics greatly influence attachment and growth of cells on biomaterials. Biocompatible polymers like PLA have been widely used as scaffold materials for tissue engineering and implantable devices, but the lack of cell recognition sites, hydrophobicity, and low surface energy lead to bad cell affinity for these polymers, which limit their usage. Plasma surface treatment, followed by surface functionalization with cationic groups, has shown to greatly enhance biomimetic properties of PLA and the consequent affinity for the cells.[33] Additionally, it has been shown that gas-plasma-treated PLA scaffolds have the potential to serve as angiogenic scaffolds. Prior work with endothelial cells on oxygen plasma treated PLA scaffolds has shown increased cell proliferation over 4–6 days and increased angiogenesis in vivo at 12 days.[34] This characteristic could be very useful for potential clinical application, permitting a better vascularization of PLA implanted devices used as cell reservoirs.

Xia et al. showed rapid endothelialization of plasma treated PLA with functionalized –COOH groups to link gelatin or chitosan, while Zhu et al. showed similar results through aminolyzed PLA.[35,36] A possible advantage of polymeric PLA implants is the local lactate release after degradation, which seems to improve angiogenesis and cutaneous wound healing in different mouse strains.[37]

To house ILIPAs and support their graft while promoting rapid vascularization, the NGs were fabricated with

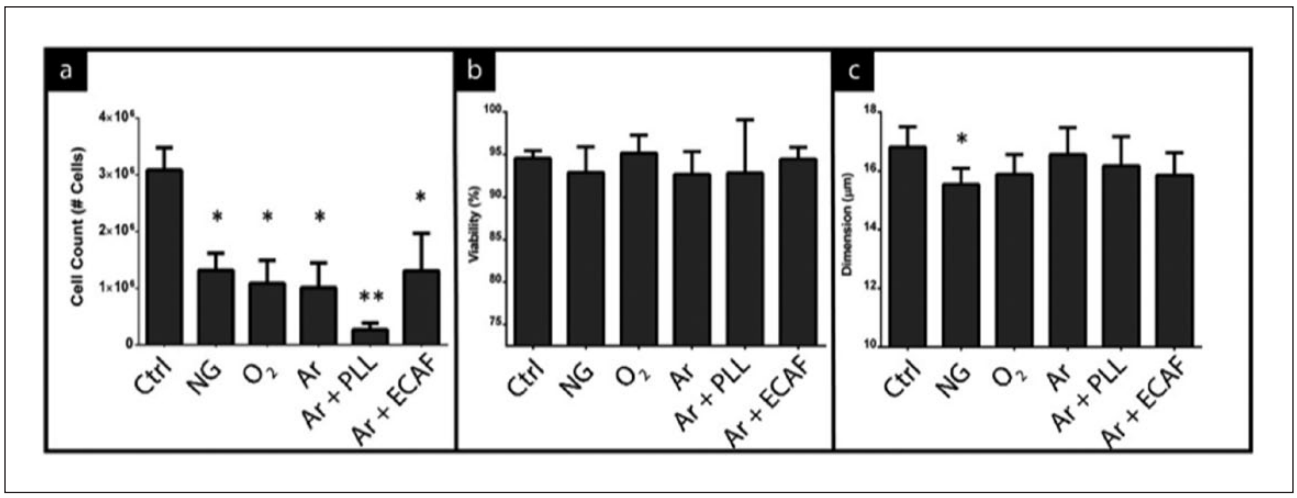


Figure 7. Effect of different polylactic acid surface modification techniques on (a) HUVEC viability, (b) growth, and (c) dimension. *$p < 0.05$; **$p < 0.001$.

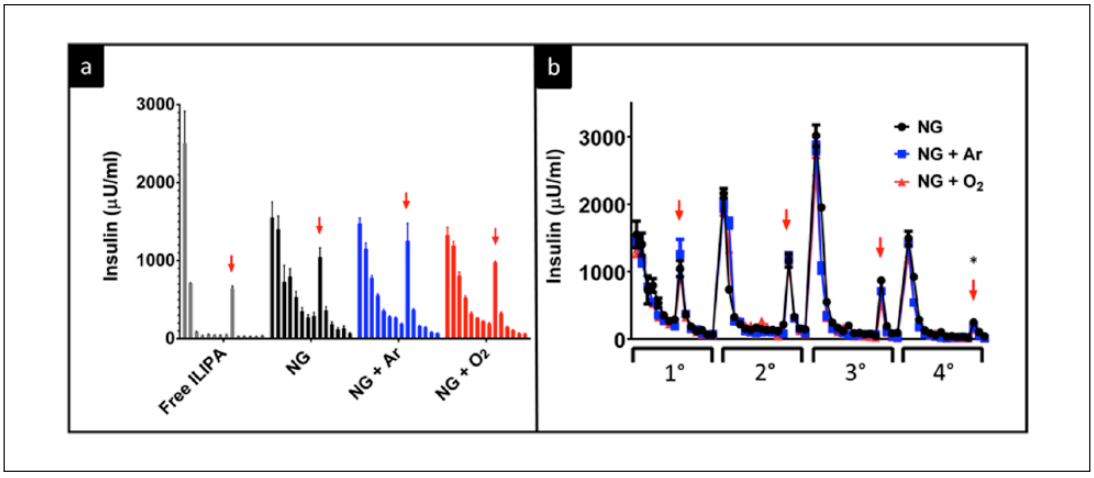


Figure 8. Effect of nanogland and surface modifications on ILIPAs' insulin secretions per ILIPA after glucose stimulation during (a) the first week of culturing and (b) over a 4-week experiment. Overnight peaks are marked by red arrows.

microchambers connected to the outside by an array of square microchannels with a 150 μm × 150 μm cross section, 50 μm in length. Previous works showed that for a successful glucose response, it is fundamental to recreate a physiological-like environment keeping cell aggregates in close proximity, but separate from each other to stimulate ingrowth of vessels under hypoxic stimuli.[38,39] With the microchamber structure, the NG houses one or few ILIPAs or islets inside each chamber avoiding clustering.

Nevertheless, further studies are needed to prove the effectiveness of this geometry, considering that endothelial cells are highly influenced in their behavior and growth properties by the geometry of the substrate.[40]

Similarly, the rigidity of the substrate has a profound influence on in vivo function. PLA scaffold rigidity is several orders of magnitude higher than the one present in tissue (>10^3 vs 1–100 kPa). Although increasing evidence indicates that cell function maybe dramatically affected by non-physiological rigidity,[41] HUVECs and ILIPA viability and morphology were not affected by NGs in vitro. A possible alternative for helping the vascularization process, reducing the rigidity, could be to use more flexible and biocompatible polymers like polycaprolactone (PCL) or print vessel-like structures in hydrogel materials.[42,43]

A major challenge in transplantation is the induction of donor specific tolerance. Recently the Food and Drug Administration (FDA) approved a CTLA-4Ig fusion protein that blocks the co-stimulatory receptor CD28 and B7 interactions, critical to T cell activation for clinical use in kidney transplantation.[44] A localized delivery of immunomodulator drugs in the vicinity of transplanted tissue, which will protect the transplant from immune rejection and at the same time eliminate the adverse effects associated with systemic immunosuppression, is the ideal choice

in islet/beta cell transplantation. Based on our group's extensive expertise with implantable drug delivery systems with microfabricated nanochannels, which have shown to achieve constant and sustained delivery of various therapeutics including testosterone, leuprolide, interferon, lysozyme, genotropin, and octreotide in several animal models for periods ranging from 1–6 months,[45–49] it is possible to incorporate a local sustained delivery of immunomodulators in the NG.

ILIPAs, either free or in NGs, did not show a measurable acute response to high glucose as a secretogogue, likely due to the lack of insulin storage granules in the ILIPA construct. However, all groups demonstrated very consistent low-level insulin production throughout the testing period and as such, may prove clinically useful as a replacement source of basal levels of insulin. All tissues tested resulted in a basal insulin level of 0.012–0.072 μU insulin per ILIPA (data not shown). An interesting observation was that free ILIPAs showed a quicker reduction in insulin release than those housed in NGs, presumably due to insulin accumulation in the PL gel matrix in the latter. Also, ILIPA overnight incubation in NGs produced higher insulin spikes. In translating these results to clinically relevant models, it would be interesting to observe vascularization, innervation, and immunological response to the encapsulated ILIPAs in murine and other animal models of diabetes, and their long-term effectiveness in maintaining euglycemia, reducing disease progression, and preventing associated complications.

Conclusion

This work demonstrates the generation of insulin-producing cells from human BM-MSCs capable of prolonged and sustained in vitro insulin production. The ILIPAs can be generated autologously, and while they do not provide a prompt insulin response to secretogogues, we demonstrate prolonged and sustained in vitro production of insulin that could provide a consistent basal level of insulin in a transplant scenario. Furthermore, we designed and developed a biomimetic NG encapsulation system suitable for long-term cell replacement therapy with islets, ILIPAs, or other insulin-producing cells. This construct could be useful to test the effect of different materials, surface modifications, and matrices on pancreatic cells properties, such as cell viability, glucose response, and insulin secretion under different stress conditions, localized angiogenesis, and immune-tolerance induction. Our NG could potentially overcome many of the hurdles of current islet transplantation strategies. Moreover, by improving the 3D printing set up and pairing with new cell electrospinning techniques, it is possible to print other 3D organotypic scaffolds to test the growth of different cell lines suitable for other clinical applications.[50,51] Further advances in the stem cell field and encapsulation technology may result in the ultimate goal of developing a true replacement of pancreatic endocrine function through a bioartificial pancreas.

Acknowledgements

The authors express their sincere gratitude to the Vivian L. Smith Foundation for the support and the Methodist Physician Organization, which made this investigation possible. Pancreata were provided by LifeGift Organ Procurement Organization, Houston, TX. Some of the research islets were provided by the Integrated Islet Distribution Program (City of Hope, Duarte, CA). The authors would like to thank Dr Jianhua Gu of the Imaging Suite of Houston Methodist Hospital for his assistance in preparing samples for SEM observations and his help in using the scanning electron microscope. Omaima M Sabek and Marco Farina are co-first authors and Ahmed O Gaber and Alessandro Grattoni are co-senior authors.

Declaration of conflicting interests

The author(s) declared no potential conflicts of interest with respect to the research, authorship, and/or publication of this article.

Funding

The author(s) received no financial support for the research, authorship, and/or publication of this article.

Supplemental material

The online figures and tables are available at http://tej.sagepub.com/supplemental

References

1. *Key findings 2014*. International Diabetes Federation, 2015. http://www.diabetesatlas.org
2. Pagliuca FW and Melton DA. How to make a functional beta-cell. *Development* 2013; 140: 2472–2483.
3. Kahn SE, Cooper ME and Del Prato S. Pathophysiology and treatment of type 2 diabetes: perspectives on the past, present, and future. *Lancet* 2014; 383: 1068–1083.
4. De Ferranti SD, de Boer IH, Fonseca V, et al. Type 1 diabetes mellitus and cardiovascular disease: a scientific statement from the American Heart Association and American Diabetes Association. *Circulation* 2014; 130: 1110–1130.
5. Borowiak M and Melton DA. How to make beta cells? *Curr Opin Cell Biol* 2009; 21: 727–732.
6. Bellin MD, Balamurugan AN, Pruett TL, et al. No islets left behind: islet autotransplantation for surgery-induced diabetes. *Curr Diab Rep* 2012; 12: 580–586.
7. Barton FB, Rickels MR, Alejandro R, et al. Improvement in outcomes of clinical islet transplantation: 1999–2010. *Diabetes Care* 2012; 35: 1436–1445.
8. Pagliuca FW, Millman JR, Gürtler M, et al. Generation of functional human pancreatic β cells in vitro. *Cell* 2014; 159: 428–439.
9. Scharp DW and Marchetti P. Encapsulated islets for diabetes therapy: history, current progress, and critical issues requiring solution. *Adv Drug Deliv Rev* 2014; 67–68: 35–73.

10. Lasprilla AJR, Martinez GAR, Lunelli BH, et al. Poly-lactic acid synthesis for application in biomedical devices—a review. *Biotechnol Adv* 30: 321–328.
11. Wang S, Cui W and Bei J. Bulk and surface modifications of polylactide. *Anal Bioanal Chem* 2005; 381: 547–556.
12. Ricordi C, Lacy PE and Scharp DW. Automated islet isolation from human pancreas. *Diabetes* 1989; 38(Suppl. 1): 140–142.
13. Fraga DW, Sabek O, Hathaway DK, et al. A comparison of media supplement methods for the extended culture of human islet tissue. *Transplantation* 1998; 65: 1060–1066.
14. Gabr MM, Zakaria MM, Refaie AF, et al. Insulin-producing cells from adult human bone marrow mesenchymal stem cells control streptozotocin-induced diabetes in nude mice. *Cell Transplant* 2013; 22: 133–145.
15. Udvardi MK, Czechowski T and Scheible W-R. Eleven golden rules of quantitative RT-PCR. *Plant Cell* 2008; 20: 1736–1737.
16. Buchwald P, Wang X, Khan A, et al. Quantitative assessment of islet cell products: estimating the accuracy of the existing protocol and accounting for islet size distribution. *Cell Transplant* 2009; 18: 1223–1235.
17. Calne RY, Gan SU and Lee KO. Stem cell and gene therapies for diabetes mellitus. *Nat Rev Endocrinol* 2010; 6: 173–177.
18. Ciceri F and Piemonti L. Bone marrow and pancreatic islets: an old story with new perspectives. *Cell Transplant* 2010; 19: 1511–1522.
19. Gabr MM, Sobh MM, Zakaria MM, et al. Transplantation of insulin-producing clusters derived from adult bone marrow stem cells to treat diabetes in rats. *Exp Clin Transplant* 2008; 6: 236–243.
20. Jiang F-X, Stanley EG, Gonez LJ, et al. Bone morphogenetic proteins promote development of fetal pancreas epithelial colonies containing insulin-positive cells. *J Cell Sci* 2002; 115: 753–760.
21. Fujimoto K and Polonsky KS. Pdx1 and other factors that regulate pancreatic beta-cell survival. *Diabetes Obes Metab* 2009; 11(Suppl. 4): 30–37.
22. Chandra V, Albagli-Curiel O, Hastoy B, et al. RFX6 regulates insulin secretion by modulating Ca2+ homeostasis in human β cells. *Cell Rep* 2014; 9: 2206–2218.
23. McCulloch LJ, van de Bunt M, Braun M, et al. GLUT2 (SLC2A2) is not the principal glucose transporter in human pancreatic beta cells: implications for understanding genetic association signals at this locus. *Mol Genet Metab* 2011; 104: 648–653.
24. Bennett K, James C and Hussain K. Pancreatic β-cell KATP channels: hypoglycaemia and hyperglycaemia. *Rev Endocr Metab Disord* 2010; 11: 157–163.
25. Gloyn AL, Siddiqui J and Ellard S. Mutations in the genes encoding the pancreatic beta-cell KATP channel subunits Kir6.2 (KCNJ11) and SUR1 (ABCC8) in diabetes mellitus and hyperinsulinism. *Hum Mutat* 2006; 27: 220–231.
26. Fossett E, Khan WS, Longo UG, et al. Effect of age and gender on cell proliferation and cell surface characterization of synovial fat pad derived mesenchymal stem cells. *J Orthop Res* 2012; 30: 1013–1018.
27. Shapiro AMJ, Ricordi C, Hering BJ, et al. International trial of the Edmonton protocol for islet transplantation. *N Engl J Med* 2006; 355: 1318–1330.
28. Lim F and Sun AM. Microencapsulated islets as bioartificial endocrine pancreas. *Science* 1980; 210: 908–910.
29. Sabek OM, Ferrati S, Fraga DW, et al. Characterization of a nanogland for the autotransplantation of human pancreatic islets. *Lab Chip* 2013; 13: 3675–3688.
30. Desai TA, Hansford DJ and Ferrari M. Micromachined interfaces: new approaches in cell immunoisolation and biomolecular separation. *Biomol Eng* 2000; 17: 23–36.
31. Desai TA, Chu WH, Rasi G, et al. Microfabricated biocapsules provide short-term immunoisolation of insulinoma xenografts. *Biomed Microdevices* 1999; 1: 131–138.
32. Borowiak M. The new generation of beta-cells: replication, stem cell differentiation, and the role of small molecules. *Rev Diabet Stud* 2010; 7: 93–104.
33. Shen H, Hu X, Yang F, et al. Combining oxygen plasma treatment with anchorage of cationized gelatin for enhancing cell affinity of poly(lactide-co-glycolide). *Biomaterials* 2007; 28: 4219–4230.
34. Polan JL, Morse B, Wetherold S, et al. VEGF analysis induced by endothelialized gas-plasma treated D,L-PLA scaffolds. *Cardiovasc Radiat Med* 3: 176–182.
35. Xia Y, Boey F and Venkatraman SS. Surface modification of poly(L-lactic acid) with biomolecules to promote endothelialization. *Biointerphases* 2010; 5: FA32–FA40.
36. Zhu Y, Gao C, Liu X, et al. Immobilization of biomacromolecules onto aminolyzed poly(L-lactic acid) toward acceleration of endothelium regeneration. *Tissue Eng* 10: 53–61.
37. Porporato PE, Payen VL, De Saedeleer CJ, et al. Lactate stimulates angiogenesis and accelerates the healing of superficial and ischemic wounds in mice. *Angiogenesis* 2012; 15: 581–592.
38. Folkman J. Tumor angiogenesis: therapeutic implications. *N Engl J Med* 1971; 285: 1182–1186.
39. Jabs N, Franklin I, Brenner MB, et al. Reduced insulin secretion and content in VEGF-a deficient mouse pancreatic islets. *Exp Clin Endocrinol Diabetes* 2008; 116(Suppl. 1): S46–S49.
40. Huang NF, Okogbaa J, Lee JC, et al. The modulation of endothelial cell morphology, function, and survival using anisotropic nanofibrillar collagen scaffolds. *Biomaterials* 2013; 34: 4038–4047.
41. Gilbert PM, Havenstrite KL, Magnusson KEG, et al. Substrate elasticity regulates skeletal muscle stem cell self-renewal in culture. *Science* 2010; 329: 1078–1081.
42. Hinton TJ, Jallerat Q, Palchesko RN, et al. Three-dimensional printing of complex biological structures by freeform reversible embedding of suspended hydrogels. *Sci Adv* 2015; 1: e1500758–e1500758.
43. Kolesky DB, Truby RL, Gladman AS, et al. 3D bioprinting of vascularized, heterogeneous cell-laden tissue constructs. *Adv Mater* 2014; 26: 3124–3130.
44. Kirk AD, Harlan DM, Armstrong NN, et al. CTLA4-Ig and anti-CD40 ligand prevent renal allograft rejection in primates. *Proc Natl Acad Sci U S A* 1997; 94: 8789–8794.

45. Ferrati S, Fine D, You J, et al. Leveraging nanochannels for universal, zero-order drug delivery in vivo. *J Control Release* 2013; 172: 1011–1019.
46. Grattoni A, Fine D, Zabre E, et al. Gated and near-surface diffusion of charged fullerenes in nanochannels. *ACS Nano* 2011; 5: 9382–9391.
47. Ferrati S, Nicolov E, Zabre E, et al. The nanochannel delivery system for constant testosterone replacement therapy. *J Sex Med* 2015; 12: 1375–1380.
48. Sih J, Bansal SS, Filippini S, et al. Characterization of nanochannel delivery membrane systems for the sustained release of resveratrol and atorvastatin: new perspectives on promoting heart health. *Anal Bioanal Chem* 2013; 405: 1547–1557.
49. Celia C, Ferrati S, Bansal S, et al. Sustained zero-order release of intact ultra-stable drug-loaded liposomes from an implantable nanochannel delivery system. *Adv Healthc Mater* 2014; 3: 230–238.
50. Jayasinghe SN, Qureshi AN and Eagles PAM. Electrohydrodynamic jet processing: an advanced electric-field-driven jetting phenomenon for processing living cells. *Small* 2006; 2: 216–219.
51. Townsend-Nicholson A and Jayasinghe SN. Cell electrospinning: a unique biotechnique for encapsulating living organisms for generating active biological microthreads/scaffolds. *Biomacromolecules* 2006; 7: 3364–3369.